

# Flow cytometric assessment of specific leucine incorporation in the open Mediterranean

A. Talarmin<sup>1,2,3,4</sup>, F. Van Wambeke<sup>1,2</sup>, P. Catala<sup>3,4</sup>, C. Courties<sup>3,5</sup>, and P. Lebaron<sup>3,4</sup>

<sup>1</sup>Université de la Méditerranée, Centre d'Océanologie de Marseille, Case 901, Campus de Luminy, 13288 Marseille, France

<sup>2</sup>CNRS/INSU, UMR 6117, LMGEM, Case 901, Campus de Luminy, 13288 Marseille, France

<sup>3</sup>UPMC Univ Paris 06, Laboratoire ARAGO – Observatoire Océanologique, 66651 Banyuls/mer, France

<sup>4</sup>CNRS, UMR 7621, LOMIC, Observatoire Océanologique, 66651 Banyuls/mer, France

<sup>5</sup>CNRS, UMS 2348, Observatoire Océanologique, 66651, Banyuls/mer, France

Received: 26 July 2010 – Published in Biogeosciences Discuss.: 30 August 2010

Revised: 14 January 2011 – Accepted: 25 January 2011 – Published: 7 February 2011

**Abstract.** The surface of the Mediterranean Sea is a low-phosphate-low-chlorophyll marine area where marine heterotrophic prokaryotes significantly contribute to the biogeochemical cycles of all biogenic elements such as carbon, notably through the mineralization of dissolved organic compounds. Cell-specific leucine incorporation rates were determined in early summer in the open stratified Mediterranean Sea. The bulk leucine incorporation rate was on average  $5 \pm 4 \text{ pmol leu l}^{-1} \text{ h}^{-1}$  ( $n = 30$ ). Cell-specific  $^3\text{H}$ -leucine incorporation rates were assayed using flow cytometry coupled to cell sorting. Heterotrophic prokaryotes (Hprok) were divided into cytometric groups according to their side scatter and green fluorescence properties: high nucleic acid containing cells (HNA) with high scatter (HNA-hs) and low scatter (HNA-ls) and low nucleic acid containing cells (LNA). Cell-specific leucine incorporation rates of these cytometric groups ranged from 2 to 54, 0.9 to 11, and 1 to  $12 \times 10^{-21} \text{ mol cell}^{-1} \text{ h}^{-1}$ , respectively. LNA cells represented 45 to 63% of the Hprok abundance, and significantly contributed to the bulk leucine incorporation rates, from 12 to 43%. HNA/LNA ratios of cell-specific leucine incorporation were on average  $2.0 \pm 0.7$  ( $n = 30$ ). In surface layers (from 0 m down to the deep chlorophyll depth, DCM), cell-specific rates of HNA-hs were elevated (7 and 13 times greater than LNA and HNA-ls, respectively). Nevertheless, on average HNA-hs (26%) and LNA (27%) equally contributed to the bulk leucine incorporation in these layers. *Prochlorococcus* cells were easily sorted near the DCM and displayed cell-specific leucine incorporation rates ranging from 3 to  $55 \times 10^{-21} \text{ mol leu cell}^{-1} \text{ h}^{-1}$ , i.e. as high as

HNA-hs'. These sorted groups could therefore be defined as key-players in the process of leucine incorporation into proteins. The mixotrophic features of certain photosynthetic prokaryotes and the high contribution of LNA cells to leucine incorporation within the microbial communities of the Mediterranean could be reinforced.

## 1 Introduction

Flow cytometry (FCM) enabled 2 groups of aquatic heterotrophic prokaryotes (Hprok) to be differentiated and thoroughly explored according to their cellular nucleic content: i.e. low nucleic acid containing cells (LNA) and high nucleic acid containing cells (HNA, Li et al., 1995; Troussellier et al., 1995). Radiolabeling coupled to cell sorting has been shown to be a powerful technique in assessing the cell-specific activities of HNA and LNA groups. On a volumetric basis, the role of HNA cells generally dominates bulk  $^3\text{H}$ -leucine incorporation rates in a variety of environments, due to their high cell-specific leucine incorporation rates, larger than those of LNA cells (Servais et al., 1999, 2003; Lebaron et al., 2001; Longnecker et al., 2005).

The view that LNA cells are dormant, inactive, or dead cells has been called into question as they have been shown to exhibit substantial heterotrophic activity, being able to assimilate leucine, methionine and thymidine (e.g. Longnecker et al., 2005, 2006; Mary et al., 2006, 2008b; Zubkov et al., 2006; Hill et al., 2010). LNA cells also play a role in the microbial food web, as the growth and grazing of LNA cells are more or less balanced (Scharek and Latasa, 2007). This discrepancy could be related to a high phylogenetic diversity of the groups sampled, and/or to varying biotic and



Correspondence to: A. Talarmin  
([agathe.talarmin@univmed.fr](mailto:agathe.talarmin@univmed.fr))

abiotic factors driving the dynamics and activity of the bacterioplankton. Indeed, molecular fingerprinting or FISH techniques applied to the sorted fractions showed that HNA and LNA cells could reflect either comparable or very different diversity patterns (Zubkov et al., 2001, 2002; Servais et al., 2003; Longnecker et al., 2005; Mary et al., 2006). Bouvier et al. (2007) suggested that cells were dynamically evolving with possible exchanges between the 2 groups.

Among the biotic and abiotic factors governing the dynamics and activity of HNA and LNA cells, the most commonly examined are trophic gradients (depth, coast-offshore), explored using the relationships with chlorophyll, primary production or nutrients (Bouvier et al., 2007, and references therein). Generally, these studies show that cell-specific nucleic acid content does not appear to be a good proxy for determining levels of bacterial activity in open and oligotrophic systems. Changes in the nature and quantity of resources and grazers affect both cytometric groups (Servais et al., 1999; Nishimura et al., 2005; Longnecker et al., 2010). Temperature selectively affects some groups along the water column, longitudinal gradients, or seasons (Longnecker et al., 2006; Moran and Calvo-Díaz, 2009), but the identification of a single factor driving HNA and LNA cell distribution is difficult, due to the simultaneous variation of biogeochemical variables along trophic gradients (Moran et al., 2010).

The oligotrophic to ultra-oligotrophic status of the open Mediterranean Sea has important consequences on dominance and functioning of the microbial food web, with picoplankton dynamics being largely influenced by the availability of N and P in surface waters (Siokou-Frangou et al., 2010). Microbial food webs are dominated by small-sized organisms, including Hprok, whose carbon demand often exceeds phytoplankton primary production (Lemée et al., 2002).

It is therefore important to understand how LNA and HNA groups share C fluxes across the open Mediterranean Sea. Few studies have been published to date on this topic (Vaqué et al., 2001; Scharek and Latasa, 2007), and the technique using radiolabeling coupled to flow sorting has only been carried out in coastal Mediterranean Sea samples in pioneer work by Servais et al. (1999, 2003) and Lebaron et al. (2001, 2002).

The aim of this study was to quantify fluxes of leucine incorporation on a volumetric and single-cell basis, using flow sorting. Fluxes were determined in the 0–200 m layer at 5 selected stations and in 1.5–4 day amendment experiments, in order to check for any possible control on biological processes by nutrients. In addition, Hprok groups, *Synechococcus* (Syn) and *Prochlorococcus* (Proc) cyanobacteria were also analysed at selected stations, as these 2 latter groups are the main primary producers in the Mediterranean Sea (Hagström et al., 1988). This study constitutes a first assessment of specific leucine incorporation activity in picoplanktonic groups in the Mediterranean Sea, with a particular focus on vertical variability.

## 2 Material and methods

### 2.1 Study area and sample collection

This work was carried out during the “BOUM” cruise on the R/V *Atalante* in June–July 2008. The cruise was planned as a longitudinal transect of stations across the Mediterranean Sea (Fig. 1, see also Moutin et al., 2011). Water samples were collected using a rosette equipped with  $24 \times 12$ -l Niskin bottles mounted on a CTD system. At 5 stations (St. 25, A, 21, B and C, from West to East, Fig. 1), samples were collected between 0 and 200 m for the determination of bulk and cell-specific leucine incorporation rates in the prokaryotes, and for cell enumeration. Total chlorophyll-*a* (TChl-*a*) and nutrients (phosphate, nitrate, nitrite) were determined (Crombet et al., 2010; Pujol-Pay et al., 2010). Deep chlorophyll maximum depth was obtained from the vertical plot of in vivo fluorescence detected by the fluorescence sensor (Seabird). LNA and HNA cell distribution and total heterotrophic prokaryotic production (BP) along the BOUM transect are presented in Van Wambeke et al. (2010).

### 2.2 Enrichment experiments

Two experiments have been reported: at station B, surface water (8 m) was dispensed into a series of 20-l polycarbonate bottles. Under in situ simulated light and temperature conditions (using neutral screens in large on-deck tanks filled with running surface seawater), triplicate bottles of each treatment (C: unamended control, N: +1.6  $\mu\text{M}$  ammonium, P: +0.1  $\mu\text{M}$  phosphate, NP: + both nutrients) were followed over 4 days. Subsamples were periodically taken for Hprok abundance and BP (Tanaka et al., 2010). At St. 21, seawater from 5 m was incubated under the same temperature and light conditions as for St. B, but the samples were incubated in 60-ml flasks with different nutrient combinations (C: unamended control, P: +0.25  $\mu\text{M}$  phosphate, N: +1  $\mu\text{M}$  nitrate + 1  $\mu\text{M}$  ammonium, G: +10  $\mu\text{M}$  C-glucose and a NPG combination: addition of the 4 nutrients). The samples were incubated for 1.5 days. Abundance and specific leucine incorporation rates were determined at the end of each experiment.

### 2.3 Onboard sample treatment

For delayed cell enumeration, 4-ml seawater samples were transferred into cryovials, and fixed onboard using formaldehyde (2% final concentration). After 10 min at room temperature in the dark, samples were frozen in liquid nitrogen for 24 h and finally, stored at  $-80^\circ\text{C}$  until processed on shore, 2 months after the cruise.

For measurements of bulk and cell-specific leucine incorporation rates, 4-ml triplicate samples were incubated (for each depth and treatment) using a 12 nM final concentration of  $^3\text{H}$ -leucine (Perkin Elmer Life Science, specific activity  $115.4 \text{ Ci mmol}^{-1}$ ), in the dark, at simulated in situ temperature. This concentration has been previously shown to be

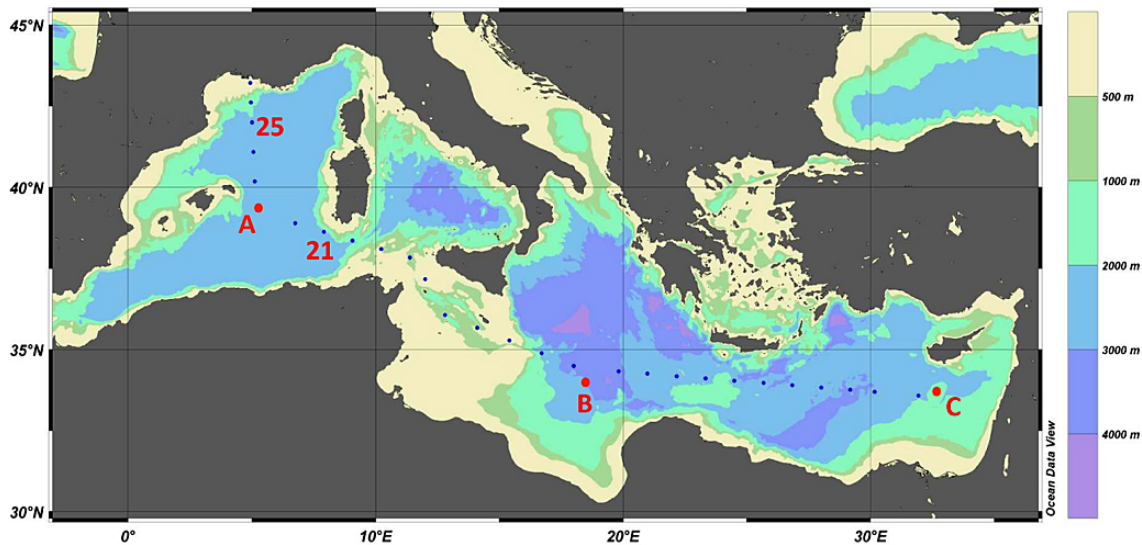


**Fig. 1.** Location of the BOUM transect and sampling sites: stations St. 25, A, 21, B and C from West to East.

saturation for the bulk measurements routinely carried out on board using the centrifuge technique (Van Wambeke et al., 2010). One of the 3 aliquots was used as a control, having been killed by the addition of filtered paraformaldehyde (PFA, 2% final concentration) 10 min before adding the radiolabeled leucine. Incubations lasted up to 5 h (in the linear phase of incorporation) to ensure sufficient labelling before flow sorting. Following incubation, samples were killed with PFA (2% final concentration), put briefly in liquid nitrogen for 15 min and stored frozen at  $-80^{\circ}\text{C}$  until analysis on shore.

## 2.4 Flow cytometry analyses on shore

### 2.4.1 Cell enumeration

Samples were thawed at room temperature, and analysed using a FACScan or a FACSCalibur flow cytometer (BD-Biosciences), both instruments being equipped with an air-cooled argon laser (488 nm, 15 mW) and used with the same optical set and performance.

Phototrophic cells were enumerated in unstained samples with a FACScan flow cytometer, according to their right-angle light scatter properties (SSC), and their natural fluorescence from phycoerythrin and chlorophyll pigments. Abundance of heterotrophic prokaryotic groups were determined after staining with SYBR Green I (final dilution of 1/4000, Molecular probes) with a FACSCalibur flow cytometer, according to Marie et al. (2000). Data acquisition was achieved using the Cell-Quest software (BD-Biosciences) on both instruments. Fluorescent  $1.002\ \mu\text{m}$  beads (Polysciences) were systematically added to each sample analysed, as an internal standard for fluorescence and SSC. The exact volume of sam-

ple analysed was determined by measuring sample volumes before and after analysis.

### 2.4.2 Specific leucine incorporation rates of $^3\text{H}$ -radiolabeled sorts on preserved marine samples

After thawing, the duplicates were mixed so that a sufficient volume of sample could be dedicated to 3 types of measurements: (i) bulk leucine incorporation rates (see below, Sect. 2.5), (ii) flow sorting of Hprok, (iii) flow sorting of phototrophic cells. Aliquots of 3.5 ml were dedicated to the flow sorting of phototrophic cells, and we attempted to measure leucine incorporation by phototrophs. Another aliquot of 3 ml was stained with SYBR Green I (as described above) 30 min before cell sorting, so as to determine the cell-specific leucine incorporation rates of the Hprok cytometric groups. Samples were kept in the dark at  $+4^{\circ}\text{C}$  between thawing and flow sorting. A FACSAria cell sorter (BD-Biosciences) was used to analyse and to sort  $^3\text{H}$ -radiolabeled phototrophic and stained prokaryotic groups. The FACSDiva software (BD-Biosciences) was used to run the cell sorter and acquire data. Sterilized particle-free seawater passed through  $0.2\ \mu\text{m}$  (Stericap, Whatman) was used as the sheath fluid. Analysis and sorting were run using a  $70\ \mu\text{m}$  nozzle, submitted to a pressure of 85 PSI. Sorting precision mode was 0/32/0, allowing 99% of recovery. The rates of total events per second were generally below 1000 for phytoplankton, and below 2500 for Hprok sorts.

Several groups were enumerated and flow sorted: the phototrophic *Synechococcus* (Syn) and *Prochlorococcus* (Proc) cyanobacteria, few pico-/nanophytoeukaryotes (Pic), and stained heterotrophic prokaryotes (Hprok). Hprok cells were divided in several groups: cells with low (LNA) and

high nucleic acid (HNA), these being divided into 2 further groups, according to the SSC values (proxy of the size): high scatter (HNA-hs) and low scatter (HNA-ls). The “total Hprok” group (large gate including HNA-hs + HNA-ls + LNA cells) was analysed in a single sort. Cytograms of these groups obtained from an in situ sample are shown as an example in Fig. 2a, b. In the enrichment experiment from St. 21, a fifth gate was designed for HNA+ cells (Fig. 2c), characterized by similar green fluorescence as HNA cells, but with much higher SSC values.

Four, three or two sorting-ways were simultaneously used to isolate the sorted cells into different centrifuge micro-tubes (from 10 000 to 430 000 cells for Hprok groups, 500 to 20 000 cells for eukaryotes, and 500–150 000 cells for Syn and Proc). Following collection, sorted fractions were treated based on the centrifuge protocol of Smith and Azam (1992). Trichloroacetic acid (TCA) solution was added to the sorted cells to yield a final volume of 1.5 ml, and a 5% TCA final concentration. Tubes had 3 runs of centrifugation separated by rinse steps using 5% TCA and 80% ethanol, and then counted in PCS scintillation cocktail as described in Van Wambeke et al. (2010). Killed blanks were sorted using the same procedure as the incubated samples, and blank values (in dpm per cell) were subtracted from their corresponding sample. We were able to obtain significant signals for most of the sorted groups down to 200 m at all stations, with signals being at least 2-fold higher than the corresponding blank values.

Cell-specific leucine incorporation rates (thereafter “cell-specific rates”) were determined by dividing the activity of a sorted group by the associated number of sorted cells. Volumetric leucine incorporation rates (thereafter “volumetric rates”) for each sorted group were calculated by multiplying the cell-specific rate of a group by its natural abundance. Coefficient of variation of cell-specific rates between replicate sorts ( $n = 3$ , test performed on 24 occasions in different samples and groups) ranged from 2 to 18%, with an average of 7%. Total Hprok single sort was used to check signal recovery and/or effects of propagating errors by comparing total Hprok volumetric rates with the sum of the volumetric rates measured in HNA-hs, HNA-ls and LNA (“summed Hprok” volumetric rates). Volumetric rates for the total Hprok group were significantly correlated with the summed volumetric rates of the 3 groups (model II linear regression,  $r = 0.94$ ), with a slope significantly higher than 1 ( $1.28 \pm 0.08$ , data not shown). On average, summed volumetric rates for the 3 groups were lower by a factor of  $20 \pm 18\%$  ( $n = 30$ ) compared to the total Hprok volumetric rate. This 20% value lies in the upper range of the coefficient of variation obtained in the determination of cell-specific rates.

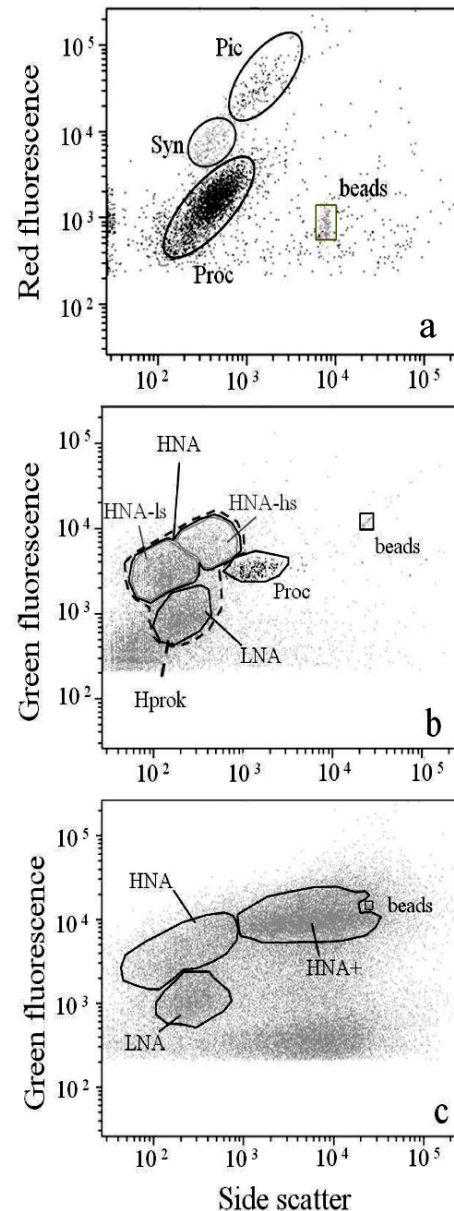


**Fig. 2.** Examples of flow cytometry biparametric plots of: **(a)** phototrophic groups discriminated by the fluorescence of their pigments and by their side scatter; **(b, c)** heterotrophic prokaryotic groups discriminated by their SYBR Green I-induced fluorescence versus their side scatter; **(b)** Heterotrophic prokaryotes and Proc (not excluded to show their localization) from an in situ sample. Sorting gates for HNA-hs, HNA-ls and LNA are shown (continuous lines), as well as limits for the total Hprok flow sorting (as a single sort, dashed line); **(c)** heterotrophic prokaryotic groups in an enrichment experiment, including HNA+ group.

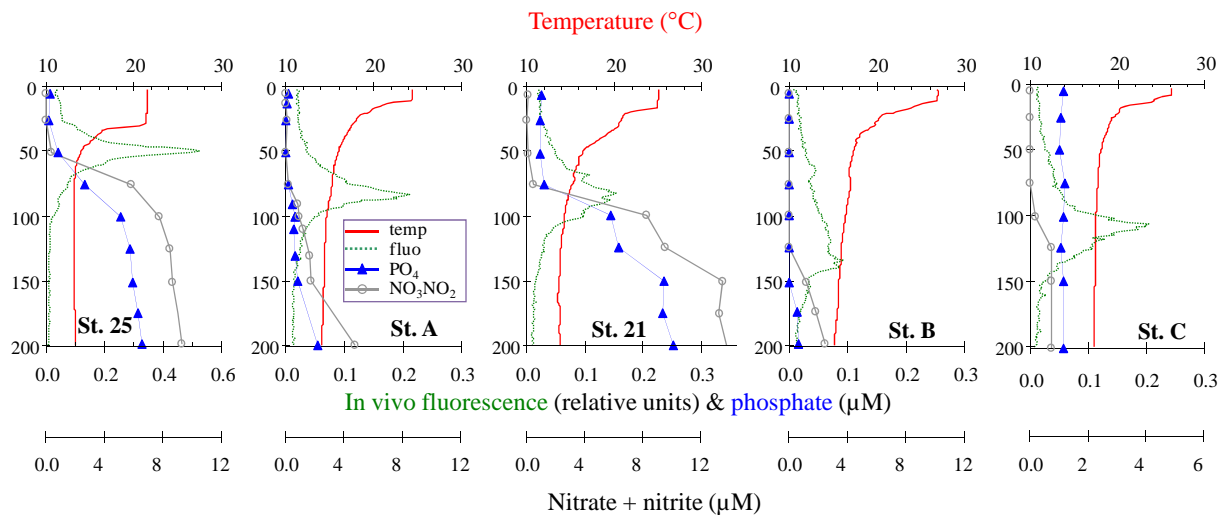


**Fig. 3.** Vertical distributions of environmental parameters: water temperature (temp, °C), in vivo fluorescence (fluo, relative units), phosphate ( $\text{PO}_4$ ) and nitrate + nitrite ( $\text{NO}_3$   $\text{NO}_2$ ) concentrations ( $\mu\text{M}$ ).

## 2.5 Bulk sea water leucine incorporation rates

After thawing a tube for further flow sorting, an aliquot of 1.5 ml was used for measuring whole seawater leucine incorporation rates (thereafter “bulk rate”). TCA was added (5% final concentration), and the centrifuge procedure was used, as for the sorted fractions. Values obtained from this bulk were used as reference values, measured using the same conditions of fixation and storage as sorted samples.

## 2.6 Statistical analyses

We conducted Pearson’s correlation analyses to examine relationships between leucine incorporation rates and environmental variables using the XLStats software. Other results are expressed as ranges minimum-maximum values measured or mean  $\pm$  standard deviation.

## 3 Results

### 3.1 Environmental parameters and microbial community structure

Vertical distribution of ancillary parameters followed a classical trend for this period of the year. Concentrations of both nitrate and phosphate were low in surface layers, often below the limit of detection. The deep chlorophyll maximum depth (DCM) deepened towards the East, from 48 m at St. 25, to 134 m at St. B (Fig. 3). The highest concentrations of TChl-*a* were observed at St. 25 ( $1.8 \mu\text{g l}^{-1}$  at the DCM and  $55 \text{ mg m}^{-2}$  throughout the 0–150 m layer). Sea-surface temperatures ranged from 21.4 to 26.8 °C (St. 25 and St. B, respectively). At stations B and C, only a slight increase in nutrient concentration was measured (Fig. 3), with

maximum values of  $0.05 \mu\text{M PO}_4$  and  $0.74 \mu\text{M NO}_2 + \text{NO}_3$  at 200 m (see Pujó Pay et al., 2010).

All flow sorted samples included (Table 1,  $n = 30$ ), Hprok abundances ranged from  $1.8$  to  $10.1 \times 10^5 \text{ cells ml}^{-1}$  with maximum values at St. 25, and the percentage of LNA cells (LNA/(HNA-hs + HNA-ls + LNA)) ranged from 45 to 63% of the total Hprok abundance. Syn abundances ranged from undetectable values to a maximum of  $77 \times 10^3 \text{ cells ml}^{-1}$  at St. 25 (40 m, Table 1). Maximum abundances of Pic were also observed at St. 25 ( $5.6 \times 10^3 \text{ cells ml}^{-1}$ ). Proc cells were generally undetectable by FCM above 25 m and their concentration peaked at less than 10 m above the DCM at all stations (maxima of  $8.1 \times 10^4 \text{ cells ml}^{-1}$  at 75 m, St. A, and  $8.2 \times 10^4 \text{ cells ml}^{-1}$  at 100 m depth, St. B).

### 3.2 Cell-specific leucine incorporation rates

#### 3.2.1 Heterotrophic prokaryotes

Cell-specific rates of HNA-hs, HNA-ls and LNA cells were pooled for all sampled stations and all depths (Fig. 4), and showed values significantly decreasing with depth (Pearson’s correlation coefficient  $r = 0.79, 0.61$  and  $0.78$ , respectively,  $p < 0.0005$ ) but increasing with temperature ( $r = 0.77, 0.50$  and  $0.86$ , respectively,  $p < 0.005$ ). No significant relationship was found between cell-specific rates and TChl-*a*, with the exception of the HNA-ls cells ( $r = 0.51, p < 0.005$ ).

HNA-hs cells always exhibited higher cell-specific rates than both HNA-ls and LNA cells (in situ data set,  $n = 30$ , HNA-hs/HNA-ls ratios ranged from 1.4 to 13.3 and HNA-hs/LNA ratios ranged from 1.9 to 6.9, Fig. 5), while cell-specific rates of HNA-ls were sometimes lower, equal or higher than those of LNA. The change in activity with depth was different between groups. Roughly, HNA-hs specific

**Table 1.** Characteristics of the biological parameters at the 5 stations. Integrated Total Chlorophyll-*a* (Int TChl-*a*: 0–150 m), number of depths sampled for flow sorting, ranges of layers sampled, and ranges of abundances and bulk leucine incorporation rates (bulk-leu) corresponding. Proc = *Prochlorococcus*, Syn = *Synechococcus*, Pic = pico + nano-phytoeukaryotes, Hprok = heterotrophic prokaryotes, ld: limit of detection.

	Int TChl- <i>a</i> (mg m <sup>-2</sup> )	Number of data	Range of depths	Proc (×10 <sup>4</sup> ml <sup>-1</sup> )	Syn (×10 <sup>3</sup> ml <sup>-1</sup> )	Pic (×10 <sup>3</sup> ml <sup>-1</sup> )	Hprok (×10 <sup>5</sup> ml <sup>-1</sup> )	Bulk leu (pmol l <sup>-1</sup> h <sup>-1</sup> )
St. 25	55	3	5, 40, 50 m	ld–2.9	0.07–77	0.05–5.6	6.6–10.1	11–17
St. A	16	9	12–200 m	ld–8.1	0.03–6.4	0.04–1.1	1.8–5.0	0.6–8.9
St. 21	21	3	5, 70, 85 m	ld–3.4	1.6–7.1	ld–0.69	5.0–5.6	4.7–9.4
St. B	16	8	5–160 m	ld–8.2	ld–6.6	0.32–1.0	2.0–5.6	0.8–9.5
St. C	23	7	5–120 m	ld–5.7	0.13–16	0.43–1.0	2.5–3.5	1.5–4.9

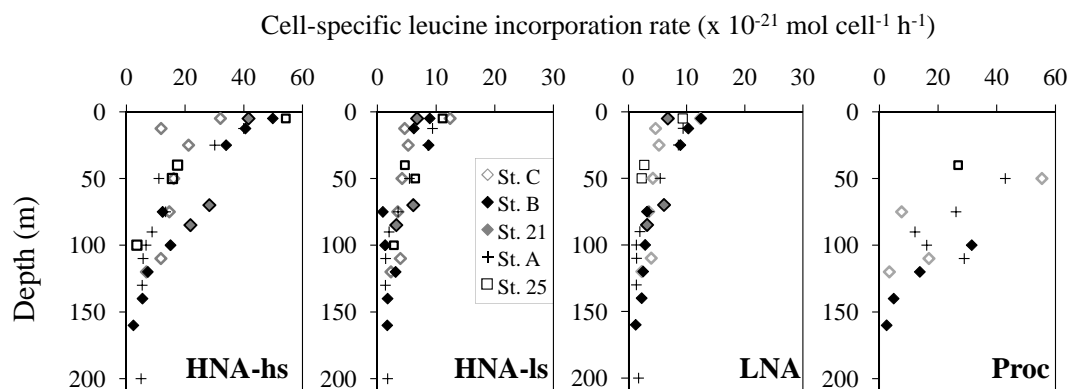


**Fig. 4.** Variability in cell-specific leucine incorporation rates for several cytomeric groups (HNA-hs, HNA-ls, LNA and Proc). Each symbol corresponds to a different profile. Note that the rate scale varies according to the cytomeric group.

rates decreased more rapidly with depth than HNA-ls, and consequently the HNA-hs/HNA-ls ratio of cell-specific rates decreased. For example at station A, cell-specific activity decreased between 5 and 200 m from  $39.9$  to  $4.9 \times 10^{-21}$  mol cell<sup>-1</sup> h<sup>-1</sup> for HNA-hs and from  $5.4$  to  $3.1 \times 10^{-21}$  mol cell<sup>-1</sup> h<sup>-1</sup> for HNA-ls, leading to strong differences in their ratios (from 7.4 at 5 m to 1.5 at 200 m, Fig. 5). For the whole data set, this ratio ranged from 2 to 13 in the surface layer, 2.4 to 3.1 at the DCM, and 1.4 to 2.1 below the DCM. Cell-specific rates of LNA were generally higher than those of HNA-ls within surface layers, but decreased more rapidly, reaching lower values than HNA-ls below the DCM. For example at St A, HNA-ls/LNA ratios ranged from 0.5 to 0.9 at the surface, 1.7 at the DCM and from 1.8 to 2.4 below the DCM (Fig. 5).

### 3.2.2 Phototrophic groups

Cell-specific rates in the phototrophic groups were examined and only sorts of more than 1000 cells, with signals 2-fold higher than their corresponding blank values were considered. Based on these criteria, there were not enough acceptable values to interpret data for Syn and Pic, and

thus we only present data obtained for *Prochlorococcus*. Proc cells contributed between 0.2 and 17% of the bacterioplankton abundance (Hprok + Syn + Proc), with an average of 7% ( $n = 15$ ). The average cell-specific rate of Proc was  $20 \pm 15 \times 10^{-21}$  mol leu cell<sup>-1</sup> h<sup>-1</sup> and this occasionally reached values as high as the surface HNA-hs cells ( $55 \times 10^{-21}$  mol leu cell<sup>-1</sup> h<sup>-1</sup> at 50 m, St. C).

## 3.3 Volumetric leucine incorporation rates

### 3.3.1 Heterotrophic prokaryotes

The volumetric leucine incorporation rates decreased significantly with depth for all sorted Hprok groups ( $p < 0.0001$  for the 3 correlations, see examples of profiles St. A, B, C, Fig. 6). The abundance contribution versus the activity contribution (Fig. 7), showed dots separated into three clusters separating HNA-hs, HNA-ls and LNA cytomeric groups. Each cluster exhibited a narrow abundance contribution range, and a wider activity contribution range with volumetric rates. LNA cells constituted a cluster lying below the 1:1 axis and characterized by the highest contribution of summed Hprok abundances (45–63%). LNA contribution to summed volumetric rates (19–58%) ranged close to those of

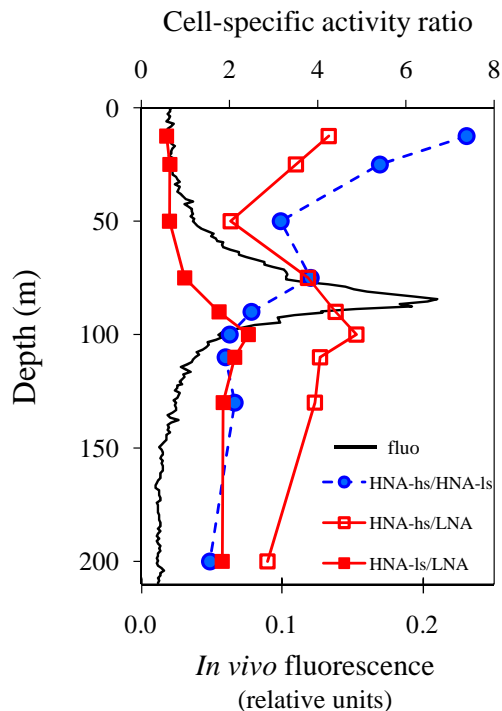


**Fig. 5.** Vertical distribution of ratios of cell-specific activities (HNA-hs to LNA, HNA-ls to LNA and HNA-hs to HNA-ls) and in vivo fluorescence at station A.

HNA-hs cells (18–65%), which clustered above the 1:1 axis. Thus, HNA-hs cells contributed less to abundance with regard to their activity. HNA-ls cells formed an intermediate cluster with a lower contribution range to summed volumetric rates than the 2 other groups (6.8–45%) although most dots overlapped the other 2 clusters in terms of activity contribution. All data of HNA-ls cells collected below the DCM layer were above the 1:1 axis. Contrary to HNA-hs cells, HNA-ls cells from the surface down to the DCM depth were less active, with regard to their abundance contribution, than the cells found below the DCM.

### 3.3.2 Phototrophic groups

Using samples from the profiles, the sum of HNA-hs, HNA-ls and LNA volumetric rates represented 36 to 108% of the bulk rates measured in the laboratory ( $64 \pm 19\%$ ,  $n = 30$ ). The missing fraction between summed volumetric rates of Hprok groups and the bulk rates (Fig. 6) was partly completed by Proc leucine incorporation. Proc volumetric rates ranged from 0.02 to  $2.6 \text{ pmol leu l}^{-1} \text{ h}^{-1}$  ( $n = 15$ ). At the DCM or just above, the contribution of Proc volumetric rate to the bulk rate increased (Fig. 6) up to 63%. The contribution of Proc appeared to be a major component of the bulk rate ( $19 \pm 16\%$ ). However, the bulk signal was not always completely recovered: excluding data corresponding to bulk rates  $< 1 \text{ pmol l}^{-1} \text{ h}^{-1}$ , summed contributions of Proc, HNA-

hs, HNA-ls and LNA represented 55 to 98% of the bulk rates (mean  $\pm$  sd:  $80\% \pm 14\%$ ).

### 3.4 Enrichment experiments

The enrichment experiment from St. 21 (left panel, Fig. 8c) demonstrated that HNA+ cell abundance increased greatly with NPG enrichment. At St. B, HNA-hs cell abundance almost doubled following NP enrichment while that of LNA decreased following N and NP additions (Fig. 8d). The addition of NPG was only tested at St. 21 but showed drastic effects on increased bulk rates. In comparison, little or no increase was observed following N only or P only enrichment (at  $< 20 \text{ pmol l}^{-1} \text{ h}^{-1}$ ), except for the N amendment (2.3-fold higher than the control). The dual combination N+P conducted at St. B gave rise to an intermediary situation with the NP enrichment treatment resulting in bulk rates of up to 4-fold higher than the control treatment (Fig. 8b). Cell-specific rates also varied depending on the nature of the amended nutrient. At St. 21, following N addition, all 3 groups responded slightly (1.4 to 2.7-fold increase). On adding NPG, HNA+ was the most responsive group (13-fold increase), followed by HNA (6-fold increase, Fig. 8e). In the experiment carried out at St. B, HNA-hs systematically showed the highest cell-specific rates, twice as high after N and NP amendments, suggesting N as the first limiting factor. The other 2 groups showed similar responses in terms of increase, but with relatively lower cell-specific rates than that of HNA-hs. However, even with LNA cells, the increase following NP enrichment was more than 2-fold higher than in the unamended control (from  $6$  to  $14 \times 10^{-21} \text{ mol cell}^{-1} \text{ h}^{-1}$ ).

## 4 Discussion

### 4.1 Importance of LNA cells in the leucine incorporation rates

This is the first data set exploring cell-specific leucine incorporation rates of HNA and LNA cells in open Mediterranean Sea waters along the euphotic zone. LNA cells incorporated significant amounts of leucine at all the stations and depths sampled ( $1.2\text{--}12.5 \times 10^{-21} \text{ mol leucine cell}^{-1} \text{ h}^{-1}$ ), and the rates were in the range of previously published values using saturating concentrations of leucine (Lebaron et al., 2002; Longnecker et al., 2006). The abundance of LNA cells reported for Pacific samples increased proportionally towards the basin station, with cell-specific rates decreasing vertically between 0 and 200 m (Longnecker et al., 2006). In the Mediterranean Sea, our data showed a greater vertical variability than longitudinal variability (Fig. 4).

The LNA participation in leucine incorporation was particularly marked in the surface layers, with contributions to total Hprok volumetric rates reaching up to 58% and contributions to bulk rates reaching up to 43%. Similar results have been previously observed in open sea compared to coastal

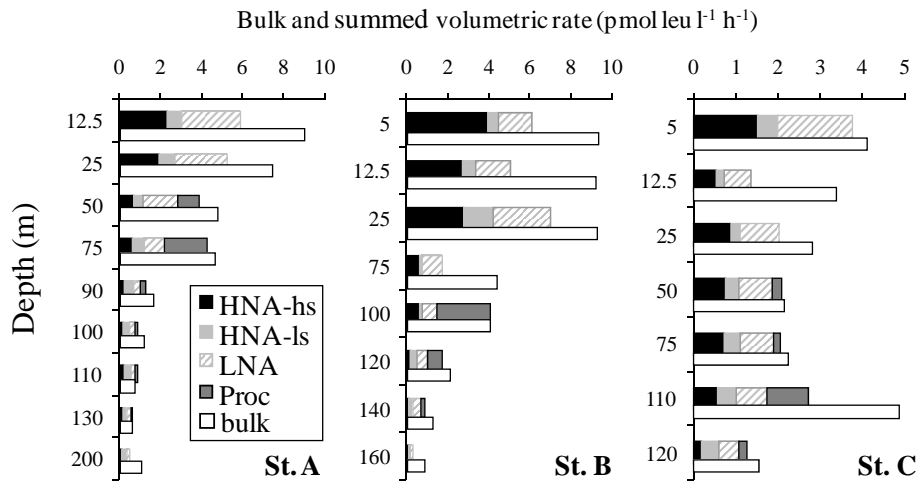


**Fig. 6.** Vertical distribution of summed volumetric rates of HNA-hs, HNA-ls, LNA and Proc compared to the bulk activity at stations St. A, B and C. Note that the depth scale varies from one profile to another.

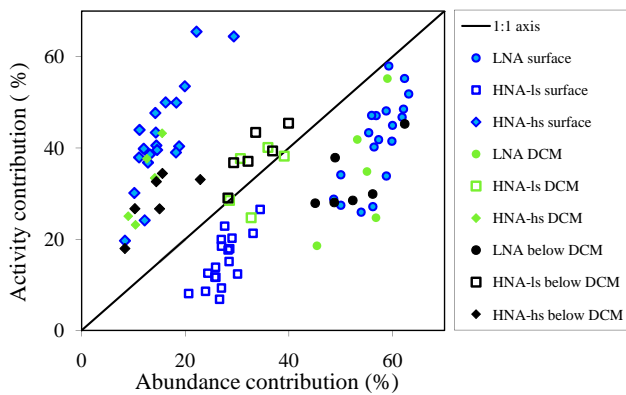


**Fig. 7.** Relationship between abundance contribution of HNA-hs, HNA-ls and LNA groups to their summed abundance and volumetric rate contribution for the same groups to their summed volumetric rates. The line represents the 1:1 axis.

and slope areas (e.g. Lebaron et al., 2001; Longnecker et al., 2005, 2006). In such oligotrophic environments, LNA cells are therefore an important dynamic group, whose role in the microbial communities and in C cycling is far from negligible. This agrees with other studies showing that significant growth rates, sometimes equal to those of HNA cells, were also measured in LNA cells (Scharek and Latasa, 2007; Williams et al., 2008). LNA cells were found to be active members of the Hprok community, not only in terms of protein synthesis, but also in cell division, as shown in groups sorted following thymidine incorporation (Longnecker et al., 2006). LNA cells in surface layers may have advantages over other groups, assuming that, like in the open Atlantic, they are dominantly represented by *Roseobacter* and SAR11 clade (Mary et al., 2006). Indeed, the potential for photo-heterotrophy was detected in SAR11 cells, providing them

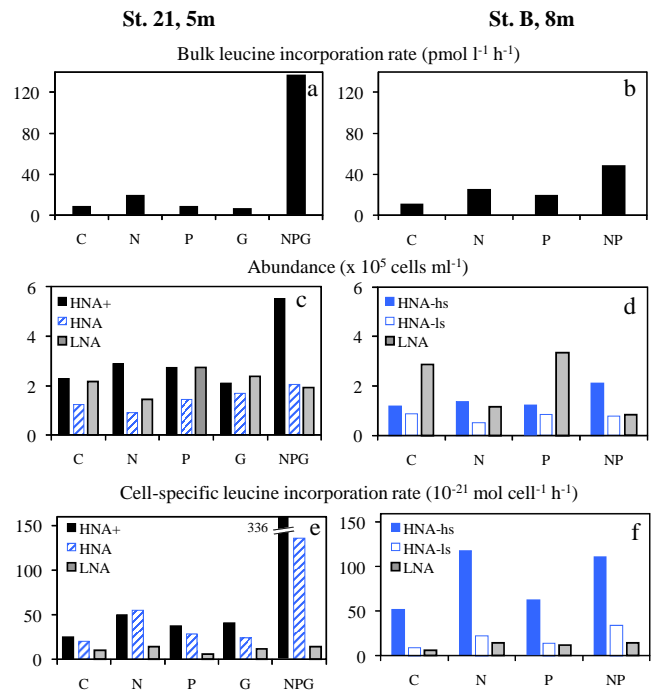


**Fig. 8.** Effects of enrichment experiments on: (a, b) bulk leucine incorporation rates, (c, d) abundances, (e, f) cell-specific leucine incorporation rates. Left: St. 21, 5 m; Right: St. B, 8 m.

with the capability of harvesting light energy (Mary et al., 2008b). Finally, in P-deficient environments, LNA cells may have the advantage of growing and dividing more efficiently than other cells because their requirements for nucleic acid synthesis are by definition lower than that of HNA cells (lake study: Nishimura et al., 2005). Our enrichment experiments showed that LNA cells were also stimulated by preventing NP nutrient limitation, further proof of their plasticity.

**Table 2.** Characteristics of the in situ Hprok cytometric groups (HNA-hs, HNA-ls and LNA): abundance, cell-specific leucine incorporation rates (cell-specific rates), contribution to Hprok volumetric rates (as the sum of HNA-hs, HNA-ls and LNA volumetric rates), and contribution to the bulk rate (whole sea water leucine incorporation rates). Data are presented as min – max (mean) values within 3 layers: “surface”: (between sea surface and the DCM depth), DCM (exact DCM depth) and “below DCM” (between DCM and the maximum layer sampled).

		Abundance ( $\times 10^5$ cells ml $^{-1}$ )	Cell-specific rates ( $\times 10^{-21}$ mol leu cell $^{-1}$ h $^{-1}$ )	Contribution to Hprok volumetric rates (%)	Contribution to the bulk rate (%)
surface ( $n = 19$ )	LNA	1.3–5.7 (2.6)	2.5–12 (6.4)	26–58 (42)	13–43 (26)
	HNA-hs	0.3–1.6 (0.7)	7.3–54 (26)	11–65 (36)	10–55 (27)
	HNA-ls	0.6–2.8 (1.3)	0.9–11 (5.0)	3–21 (13)	2.7–17 (10)
DCM ( $n = 5$ )	LNA	1.7–5.7 (2.7)	1.9–3.9 (2.7)	19–55 (35)	12–30 (19)
	HNA-hs	0.3–1.3 (0.6)	5.4–22 (13)	17–43 (28)	12–37 (19)
	HNA-ls	0.9–3.1 (1.7)	1.7–7.7 (4.6)	16–38 (28)	8.9–33 (20)
below DCM ( $n = 6$ )	LNA	0.8–2.1 (1.4)	1.2–2.3 (1.6)	28–45 (33)	14–32 (23)
	HNA-hs	0.3–0.5 (0.3)	2.3–6.8 (5.3)	14–32 (25)	12–37 (21)
	HNA-ls	0.6–1.0 (0.9)	1.7–3.9 (2.9)	28–45 (34)	11–40 (28)

#### 4.2 Large variability of HNA leucine incorporation rates

HNA-hs/HNA-ls cell-specific rate ratios could reach up to a 13-fold range, which is in accordance with previous studies. Cell-specific leucine incorporation rates of HNA were shown to vary as much as 9-fold in a single sample (Lebaron et al., 2002), depending on the regions drawn on the cytograms prior to cell sorting. Using  $^{35}\text{S}$ -labeled methionine as a tracer ( $<0.3$  nM), Zubkov et al. (2001) reported HNA-hs cell-specific assimilation rates to be 4 times higher than HNA-ls group. They also indicated that HNA-ls cell-specific leucine incorporation rates were less variable between layers than those measured in HNA-hs, and sometimes lower than those in LNA cells. Using  $^3\text{H}$ -leucine at 10 nM, our data from the Mediterranean Sea confirmed this trend, as the prokaryotic community was less heterogeneous around the DCM in terms of cell-specific rates (Fig. 4, Table 2). In accordance with such results, Scharek and Latasa (2007) found that HNA and LNA growth rates decreased at the DCM, the difference between both groups becoming insignificant.

No significant correlations were found between SSC values of HNA-hs or HNA-ls cells and their cell-specific rates, despite the higher cell-specific rates within the HNA-hs group measured in most areas. This suggests that larger cells can synthesize proteins at higher rates (compared for example to thymidine synthesis, see Longnecker et al., 2006), due to their larger protein biomass (Zubkov et al., 2001). Distinction between HNA-hs and HNA-ls cells is not always easy. Examining Hprok dynamics and community structure during a phytoplankton bloom in the North Sea, Zubkov et al. (2002) established the existence of two HNA subgroups separated after protein staining (SYPRO protein red fluorescence dye) and verified so that no such clusters were visible with DNA staining.

Because few studies investigate specific activities within HNA groups, it is difficult to compare our results with data from the literature. Thus, specific rates of HNA-hs and HNA-ls cells were used to calculate their equivalent for HNA cells as follows:

$$SA_{\text{HNA}} = \left[ (SA_{\text{HNA-ls}} \times N_{\text{HNA-ls}}) + (SA_{\text{HNA-hs}} \times N_{\text{HNA-hs}}) \right] / (N_{\text{HNA-ls}} + N_{\text{HNA-hs}})$$

where SA is the cell-specific leucine incorporation rates and N the abundance of the considered group. The range of the HNA/LNA ratios for cell-specific rates in samples  $<100$  m from slope and basin stations are 1.5–2.7 (Longnecker et al., 2006) which are comparable to our open Mediterranean Sea samples ( $2.1 \pm 0.7$ , ranging from 1.0 to 4.0). Scharek and Latasa (2007) working on a slope station of the NW Mediterranean Sea in spring, found that growth rates of HNA were significantly higher and distinct from those of LNA within surface layers, and they attributed the specificity of the surface response to coastal and/or Rhone river influences. However, we measured markedly higher HNA cell-specific rates in the surface layers at the open-sea stations, which were nevertheless located far from any river influence. Thus, other factors were responsible for the depth variability of cell-specific rates among the different groups. Indeed, differences between surface and DCM layers, in terms of habitat for Hprok, are noticeable under stratified conditions. With changing limiting factors (switch from N-P limitation to C limitation: Sala et al., 2002; Van Wambeke et al., 2002) and changes in phytoplankton populations which probably fuel different carbon resources along the water column, the result is a change in the Hprok taxonomic composition (Ghiglione et al., 2008).

#### 4.3 Effect of nutrient addition on the Hprok leucine incorporation rates

Enrichment experiments showed that leucine incorporation rates were partly nutrient-controlled, which is not uncommon in the Mediterranean Sea (Van Wambeke et al., 2002; Zohary et al., 2005; Pinhassi et al., 2006). This emphasized the bottom-up effect of either single or multiple nutrients. We further investigated the hypothesis according to which limitations could differ in distinct cytometric groups. None of the tested combinations stimulated just one group. However, we observed that nutrient additions could selectively affect the intensity of cell-specific rates. HNA cells were the most responsive, particularly HNA+ with up to 13-fold stimulation of the cell-specific rate after an NPG addition. In these experiments, abundance varied less than cell-specific rates (Fig. 8), which may be explained by a top-down control by predation and viral lysis of the most active cells (Longnecker et al., 2010). We could assume that HNA cells were partly grazed during incubation, so allowing an opportunistic group, which could be composed of HNA+, to grow rapidly. With high cell-specific rates, HNA+ cells could have an additional advantage over HNA as they are protected from grazing due to their very large size (Pfandl et al., 2004). HNA+ cells could easily develop in the 60 ml-flasks due to the expected scarcity of large-sized grazers (microzooplankton) in such a volume and this dual capacity could explain their high abundance. The low-varying cell abundance found at St. B may also be attributable to the lower stimulation of cell-specific rates when using only NP compared to using a NPG addition, and a top-down regulated community, considering the size of the microcosms (20 l) used. Indeed, Tanaka et al. (2010) showed that the addition of NP resulted in a significant increase in heterotrophic nanoflagellates at St. B along with virus and ciliates, although for these 2 latter parameters the increase was not significant due to variability within triplicate mesocosms. The outcompeting cells developing in such conditions are organisms with an “r-strategy”, as demonstrated in our experiments with HNA+ cells. This could explain the classically reported loss or shift in diversity found in other amendment experiments (Eilers et al., 2000; Schafer et al., 2000; Massana et al., 2001; Van Wambeke et al., 2009).

#### 4.4 Importance of *Prochlorococcus* in amino acid assimilation

Within the natural samples from the Mediterranean Sea, *Prochlorococcus* was able to assimilate leucine. Under dark incubation conditions, *Prochlorococcus* could be responsible for up to 63% of the total leucine incorporation into proteins, with highest contributions measured in the vicinity of the DCM. *Prochlorococcus* volumetric rates were in some cases sufficient to compensate the “unrecovered activity” observed when comparing bulk unsorted activity to the summed volumetric rates of strict Hprok groups (Fig. 5).

Significant assimilation of leucine by natural *Prochlorococcus* cells was also shown in Atlantic Ocean using a concentration of radiolabeled leucine as low as 0.8 nM (Mary et al., 2008b). As we used 12 nM leucine, it is possible that assimilation by mixotrophs could be lower under in situ conditions where natural leucine concentrations are about 0.5 nM (Mary et al., 2008b), and thus our contributions for *Prochlorococcus* could be overestimated. Indeed, in the North Atlantic, Michelou et al. (2007) observed that *Prochlorococcus* contributed up to 24% of the total leucine assimilation (added at 20 nM) and only 10% assimilation of an amino acid mixture (added at 0.5 nM concentration), whereas the opposite trend was found for *Synechococcus*. Finally, photosynthetically active radiations and UV radiations could influence the mixotrophic capacities of *Prochlorococcus* (Paerl, 1991; Michelou et al., 2007; Mary et al., 2008b; Alonso-Saez et al., 2006) and this needs further investigation, as our samples were incubated in the dark.

Mixotrophy, through amino acid uptake, gives cyanobacteria an advantage in N-limited environments (Mary et al., 2008a). The balance between photosynthesis and heterotrophic assimilation of organic molecules by *Prochlorococcus* cells may be influenced by the varying nature and/or quantity of pigmental units and also by the ecotypes present at a given depth with their metabolic ability to use nitrates and nitrites (Bouman et al., 2006; Garczarek et al., 2007; Martiny et al., 2009). Unfortunately, in the most N-depleted surface waters encountered along the transect, *Prochlorococcus* was not detected by FCM, due to their very low pigment content.

Being one of the top 3 contributors to the bulk leucine incorporation in some of our samples, this technical limitation concerning *Prochlorococcus* has one major consequence. Volumetric rates for *Prochlorococcus* measured in surface waters cannot be estimated, and therefore the Hprok contribution to the fluxes may be overestimated, by including *Prochlorococcus* cells, whose red fluorescence signal is too weak to be discarded from the Hprok group, in stained samples. Uncertainties linked to this bias in the surface samples are not quantifiable, but it can be thought that *Prochlorococcus* cells with low natural fluorescence would be counted or sorted within the HNA fraction (Fig. 2).

The capacity of these organisms to incorporate other organic molecules in the range of in situ concentrations (Mary et al., 2008b) is poorly understood. Tyrosine and some dipeptides compete for the uptake of leucine and could also be taken up by Proc cells (Mary et al., 2008a), as well as methionine (Zubkov et al., 2004). Interpreting amino acids uptake by heterotrophic and mixotrophic organisms as a single C or N flux appears slightly contentious though. Leucine and methionine are two amino acids representing sources of C, N and C, N, S, respectively. Cells may take up such substrates in cases of N and/or P depletion: indeed, it has been shown that one way to overcome P-scarcity in picophytoplankton is to synthesize sulphur-rich membrane lipids in place of the

regular phospholipids (Van Mooy et al., 2009). Thus, in the P-depleted Mediterranean, care should be taken to use  $^{35}\text{S}$ -methionine (which enhances the radioactive signal compared to  $^3\text{H}$  label) as a representative for other amino acids. More studies like this are needed in the Mediterranean using different dissolved organic carbon substrates for a careful assessment of the contribution of mixotrophs to both primary and bacterial production. The role of picoplanktonic groups in surface C cycling could then be better understood.

## 5 Conclusions

In this study we investigated specific leucine incorporation rates in the bacterioplankton of the open Mediterranean Sea, at the cellular (cell-specific) and group (volumetric) level. All heterotrophic prokaryotic groups significantly contributed to the bulk leucine incorporation rate. We measured a high vertical variability in activity and abundance, with cell-specific rates decreasing from surface to the bottom of the DCM layer, with different ranges of variation assessed in the different groups. Notably, differences between HNA-hs and HNA-ls cell-specific rates were attenuated at and below the DCM. LNA cells were shown to be active players in this flux in the Mediterranean Sea. However, most of the time HNA cells exhibited the highest contribution to the bulk rates and the lowest contribution to the summed Hprok abundance. HNA and HNA+ were the most opportunistic groups following enrichments. Significant activity was measured in *Prochlorococcus*, whose cell-specific rates could be as high as the highest HNA cell-specific rate. All these groups participated in the assimilation of labile dissolved organic carbon, and may have a major role in surface C cycling of oligotrophic oceans, where DOC is known to accumulate. Biovolume estimations and a phylogenetic survey of sorted bacterioplanktonic groups would supply consistent additional information and enable the dynamics of these organisms to be linked to the community structure, in situ and following nutrient additions.

**Acknowledgements.** This work is a contribution of the BOUM experiment (Biogeochemistry from the Oligotrophic to Ultraoligotrophic Mediterranean, <http://www.com.univ-mrs.fr/BOUM>). It was funded by the French national CNRS-INSU (LEFE-CYBER) program and the European IP SESAME (Southern European Seas: Assessing and Modelling Ecosystem Changes), EC Contract No. GOCE-036949. We acknowledge the French Research and Education Council for the Ph.D. thesis support to A. T., and express our gratitude to A. Lagaria, S. Psarra, J. Ras, M. Pujo-Pay and L. Oriol for providing TChl-*a* and nutrient data. We are grateful to T. Bentley for language corrections and the 3 anonymous referees who helped to substantially improve the manuscript, and also to the officers, crew and scientists of the BOUM cruise for helpful contribution at sea.

Edited by: C. Jeanthon



The publication of this article is financed by CNRS-INSU.

## References

- Alonso-Saez, L., Gasol, J. M., Lefort, T., Hofer, J., and Sommaruga, R.: Effect of Natural Sunlight on Bacterial Activity and Differential Sensitivity of Natural Bacterioplankton Groups in Northwestern Mediterranean Coastal Waters, *Appl. Environ. Microb.*, 72, 5806–5813, 2006.
- Bouman, H. A., Ulloa, O., Scanlan, D. J., Zwirgmaier, K., Li, W. K. W., Platt, T., Stuart, V., Barlow, R., Leth, O., Clementson, L., Lutz, V., Fukasawa, M., Watanabe, S., and Sathyendranath, S.: Oceanographic basis of the global surface distribution of *Prochlorococcus* ecotypes, *Science*, 312, 918–921, 2006.
- Bouvier, T., del Giorgio, P. A., and Gasol, J. M.: A comparative study of the cytometric characteristics of High and Low nucleic-acid bacterioplankton cells from different aquatic ecosystems, *Environ. Microbiol.*, 9, 2050–2066, 2007.
- Crombet, Y., Leblanc, K., Quéguiner, B., Moutin, T., Rimmelin, P., Ras, J., Claustre, H., Leblond, N., Oriol, L., and Pujo-Pay, M.: Deep silicon maxima in the stratified oligotrophic Mediterranean Sea, *Biogeosciences Discuss.*, 7, 6789–6846, doi:10.5194/bgd-7-6789-2010, 2010.
- Eilers, H., Pernthaler, J., and Amann, R.: Succession of marine bacteria during enrichments: a close look at cultivation-induced shifts, *Appl. Environ. Microb.*, 66, 4634–4640, 2000.
- Garczarek, L., Dufresne, A., Rousvoal, S., West, N. J., Mazard, S., Marie, D., Caustre, H., Raimbault, P., Post, A. F., Scanlan, D. J., and Partensky, F.: High vertical and low horizontal diversity of *Prochlorococcus* ecotypes in the Mediterranean Sea in summer, *FEMS Microbiol. Ecol.*, 60, 189–206, 2007.
- Ghiglione, J. F., Palacios, C., Marty, J. C., Mével, G., Labrune, C., Conan, P., Pujo-Pay, M., Garcia, N., and Goutx, M.: Role of environmental factors for the vertical distribution (0–1000 m) of marine bacterial communities in the NW Mediterranean Sea, *Biogeosciences*, 5, 1751–1764, doi:10.5194/bg-5-1751-2008, 2008.
- Hagström, A., Azam, F., Andersson, A., Wikner, J., and Ras-soulzadegan, F.: Microbial loop in an oligotrophic pelagic marine ecosystem: possible roles of cyanobacteria and nanoflagellates in the organic fluxes, *Mar. Ecol.-Prog. Ser.*, 49, 171–178, 1988.
- Hill, P. G., Zubkov, M. V., and Purdie, D. A.: Differential responses of *Prochlorococcus* and SAR11-dominated bacterioplankton groups to atmospheric dust inputs in the tropical Northeast Atlantic Ocean, *FEMS Microbiol. Lett.*, 306, 82–89, 2010.
- Lebaron, P., Servais, P., Agogue, H., Courties, C., and Joux, F.: Does the High Nucleic Acid Content of Individual Bacterial Cells Allow Us To Discriminate between Active Cells and Inactive Cells in Aquatic Systems?, *Appl. Environ. Microb.*, 67, 1775–1782, 2001.

- Lebaron, P., Servais, P., Baudoux, A. C., Bourrain, M., Courties, C., and Parthuisot, N.: Variations of bacterial-specific activity with cell size and nucleic acid content assessed by flow cytometry, *Aquat. Microb. Ecol.*, 28, 131–140, 2002.
- Lemée, R., Rochelle-Newall, E., Van Wambeke, F., Pizay, M.-D., Rinaldi, P., and Gattuso, J.-P.: Seasonal variation of bacterial production, respiration and growth efficiency in the open NW Mediterranean Sea, *Aquat. Microb. Ecol.*, 29, 227–237, 2002.
- Li, W. K. W., Jellett, J. F., and Dickie, P. M.: DNA distributions in planktonic bacteria stained with TOTO or TO-PRO, *Limnol. Oceanogr.*, 40(8), 1485–1495, 1995.
- Longnecker, K., Sherr, B. F., and Sherr, E. B.: Activity and Phylogenetic Diversity of Bacterial Cells with High and Low Nucleic Acid Content and Electron Transport System Activity in an Upwelling Ecosystem, *Appl. Environ. Microb.*, 71, 7737–7749, doi:10.1128/aem.71.12.7737-7749.2005, 2005.
- Longnecker, K., Sherr, B. F., and Sherr, E. B.: Variation in cell-specific rates of leucine and thymidine incorporation by marine bacteria with high and with low nucleic acid content off the Oregon coast, *Aquat. Microb. Ecol.*, 43, 113–125, 2006.
- Longnecker, K., Wilson, M. J., Sherr, E. B., and Sherr, B. F.: Effect of top-down control on cell-specific activity and diversity of active marine bacterioplankton, *Aquat. Microb. Ecol.*, 58, 153–165, doi:10.3354/ame01366, 2010.
- Marie, D., Simon, N., Guillou, L., Partensky, F., and Vault, D.: DNA/RNA Analysis of Phytoplankton by Flow Cytometry UNIT 11.12, *Current Protocols in Cytometry*, 2000.
- Martiny, A. C., Kathuria, S., and Berube, P. M.: Widespread metabolic potential for nitrite and nitrate assimilation among *Prochlorococcus* ecotypes, *P. Natl. Acad. Sci.*, 106, 10787–10792, doi:10.1073/pnas.0902532106, 2009.
- Mary, I., Heywood, J. L., Fuchs, B., Amann, R., Tarran, G., Burkill, P., and Zubkov, M.: SAR11 dominance among metabolically active low nucleic acid bacterioplankton in surface waters along an Atlantic meridional transect, *Aquat. Microb. Ecol.*, 45, 107–113, 2006.
- Mary, I., Garczarek, L., Tarran, G. A., Kolowrat, C., Terry, M. J., Scanlan, D. J., Burkill, P. H., and Zubkov, M. V.: Diel rhythmicity in amino acid uptake by *Prochlorococcus*, *Environ. Microbiol.*, 10, 2124–2131, 2008a.
- Mary, I., Tarran, G. A., Warwick, P. E., Terry, M. J., Scanlan, D. J., Burkill, P. H., and Zubkov, M. V.: Light enhanced amino acid uptake by dominant bacterioplankton groups in surface waters of the Atlantic Ocean, *FEMS Microbiol. Ecol.*, 63, 36–45, 2008b.
- Massana, R., Pedros-Alio, C., Casamayor, E. O., and Gasol, J. M.: Changes in marine bacterioplankton phylogenetic composition during incubations designed to measure biogeochemically significant parameters, *Limnol. Oceanogr.*, 46, 1181–1188, 2001.
- Michelou, V. K., Cottrell, M. T., and Kirchman, D. L.: Light-Stimulated Bacterial Production and Amino Acid Assimilation by Cyanobacteria and Other Microbes in the North Atlantic Ocean, *Appl. Environ. Microb.*, 73, 5539–5546, doi:10.1128/aem.00212-07, 2007.
- Moran, X. A. G. and Calvo-Díaz, A.: Single-cell vs. bulk activity properties of coastal bacterioplankton over an annual cycle in a temperate ecosystem, *FEMS Microbiol. Ecol.*, 67, 43–56, 2009.
- Moran, X. A., Calvo-Díaz, A., and Ducklow, H. W.: Total and phytoplankton mediated bottom-up control of bacterioplankton change with temperature in the NE Atlantic shelf waters, *Aquat. Microb. Ecol.*, 58, 229–239, 2010.
- Moutin, T., Van Wambeke, F., and Prieur, L.: Introduction to the Biogeochemistry from the Oligotrophic to the Ultraoligotrophic Mediterranean (BOUM) experiment, *Biogeosciences Discuss.*, in preparation, 2011.
- Nishimura, Y., Kim, C., and Nagata, T.: Vertical and Seasonal Variations of Bacterioplankton Subgroups with Different Nucleic Acid Contents: Possible Regulation by Phosphorus, *Appl. Environ. Microb.*, 71, 5828–5836, doi:10.1128/aem.71.10.5828-5836.2005, 2005.
- Paerl, H. W.: Ecophysiological and Trophic Implications of Light-Stimulated Amino Acid Utilization in Marine Picoplankton, *Appl. Environ. Microb.*, 57, 473–479, 1991.
- Pfandl, K., Posch, T., and Boenigk, J.: Unexpected Effects of Prey Dimensions and Morphologies on the Size Selective Feeding by Two Bacterivorous Flagellates (*Ochromonas* sp. and *Spumella* sp), *J. Eukaryot. Microbiol.*, 51, 626–633, doi:10.1111/j.1550-7408.2004.tb00596.x, 2004.
- Pinhassi, J., Gomez-Consarnau, L., Alonso-Saez, L., Sala, M. M., Vidal, M., Pedros-Alios, C., and Gasol, J. M.: Seasonal changes in bacterioplankton nutrient limitation and their effects on bacterial community composition in the NW Mediterranean Sea, *Aquat. Microb. Ecol.*, 44, 241–252, 2006.
- Pujo-Pay, M., Conan, P., Oriol, L., Cornet-Barthaux, V., Falco, C., Ghiglione, J.-F., Goyet, C., Moutin, T., and Prieur, L.: Integrated survey of elemental stoichiometry (C, N, P) from the Western to Eastern Mediterranean Sea, *Biogeosciences Discuss.*, 7, 7315–7358, doi:10.5194/bgd-7-7315-2010, 2010.
- Sala, M. M., Peters, F., Gasol, J. M., Pedros-Alio, C., Marassé, C., and Vaqué, D.: Seasonal and spatial variations in the nutrient limitation of bacterioplankton growth in the northwestern Mediterranean, *Aquat. Microb. Ecol.*, 27, 47–56, doi:10.3354/ame027047, 2002.
- Schafer, H., Servais, P., and Muyzer, G.: Successional changes in the genetic diversity of a marine bacterial assemblage during confinement, *Arch. Mikrobiol.*, 173, 138–145, 2000.
- Scharek, R. and Latasa, M.: Growth, grazing and carbon flux of high and low nucleic acid bacteria differ in surface and deep chlorophyll maximum layers in the NW Mediterranean Sea, *Aquat. Microb. Ecol.*, 46, 153–161, 2007.
- Servais, P., Courties, C., Lebaron, P., and Troussellier, M.: Coupling Bacterial Activity Measurements with Cell Sorting by Flow Cytometry, *Microbiol. Ecol.*, 38, 180–189, 1999.
- Servais, P., Casamayor, E. O., Courties, C., Catala, P., Parthuisot, N., and Lebaron, P.: Activity and diversity of bacterial cells with high and low nucleic acid content, *Aquat. Microb. Ecol.*, 33, 41–51, 2003.
- Siokou-Frangou, I., Christaki, U., Mazzocchi, M. G., Montresor, M., Ribera d'Alcalá, M., Vaqué, D., and Zingone, A.: Plankton in the open Mediterranean Sea: a review, *Biogeosciences*, 7, 1543–1586, doi:10.5194/bg-7-1543-2010, 2010.
- Smith, D. C. and Azam, F.: A simple, economical method for measuring bacterial protein synthesis rates in seawater using super (3)H-leucine, *Mar. Microb. Food Webs*, 6, 107–114, 1992.
- Tanaka, T., Thingstad, T. F., Christaki, U., Colombet, J., Cornet-Barthaux, V., Courties, C., Grattepanche, J.-D., Lagaria, A., Nedoma, J., Oriol, L., Psarra, S., Pujo-Pay, M., and Van Wambeke, F.: N-limited or N and P co-limited indications in the surface waters of three Mediterranean basins, *Biogeosciences Discuss.*,

- 7, 8143–8176, doi:10.5194/bgd-7-8143-2010, 2010.
- Troussellier, M., Courties, C., and Zettlmaier, S.: Flow Cytometric Analysis of Coastal Lagoon Bacterioplankton and Picophytoplankton: Fixation and Storage Effects, *Estuar. Coast. Shelf S.*, 40, 621–633, 1995.
- Van Mooy, B. A. S., Fredricks, H. F., Pedler, B. E., Dyhrman, S. T., Karl, D. M., Koblizek, M., Lomas, M. W., Mincer, T. J., Moore, L. R., Moutin, T., Rappe, M. S., and Webb, E. A.: Phytoplankton in the ocean use non-phosphorus lipids in response to phosphorus scarcity, *Nature*, 458, 69–72, 2009.
- Van Wambeke, F., Christaki, U., Giannakourou, A., Moutin, T., and Souvermerzoglou, K.: Longitudinal and vertical trends of bacterial limitation by phosphorus and carbon in the Mediterranean Sea, *Microbiol. Ecol.*, 43, 119–133, 2002.
- Van Wambeke, F., Ghiglione, J.-F., Nedoma, J., Mével, G., and Raimbault, P.: Bottom up effects on bacterioplankton growth and composition during summer-autumn transition in the open NW Mediterranean Sea, *Biogeosciences*, 6, 705–720, doi:10.5194/bg-6-705-2009, 2009.
- Van Wambeke, F., Catala, P., and Lebaron, P.: Relationships between cytometric characteristics of high and low nucleic-acid bacterioplankton cells, bacterial production and environmental parameters along a longitudinal gradient across the Mediterranean Sea, *Biogeosciences Discuss.*, 7, 8245–8279, doi:10.5194/bgd-7-8245-2010, 2010.
- Vaqué, D., Casamayor, E. O., and Gasol, J. M.: Dynamics of whole community bacterial production and grazing losses in seawater incubations as related to the changes in the proportions of bacteria with different DNA content, *Aquat. Microb. Ecol.*, 25, 163–177, doi:10.3354/ame025163, 2001.
- Williams, C. J., Lavrentyev, P. J., and Jochem, F. J.: Bottom-up and top-down control of heterotrophic bacterioplankton growth in a phosphorus-depleted subtropical estuary, Florida Bay, USA, *Mar. Ecol.-Prog. Ser.*, 372, 7–18, 2008.
- Zohary, T., Herut, B., Krom, M. D., Fauzi, C. M. R., Pitta, P., Psarra, S., Rassoulzadegan, F., Stambler, N., Tanaka, T., Thingstad, F. T., and Woodward, E. M. S.: P-limited bacteria but N and P co-limited phytoplankton in the Eastern Mediterranean – a microcosm experiment, *Deep-Sea Res. Pt. II*, 52, 3011–3023, 2005.
- Zubkov, M. V., Fuchs, B. M., Burkill, P. H., and Amann, R.: Comparison of Cellular and Biomass Specific Activities of Dominant Bacterioplankton Groups in Stratified Waters of the Celtic Sea, *Appl. Environ. Microb.*, 67, 5210–5218, 2001.
- Zubkov, M. V., Fuchs, B. M., Tarran, G. A., Burkill, P. H., and Amann, R.: Mesoscale distribution of dominant bacterioplankton groups in the northern North Sea in early summer, *Aquat. Microb. Ecol.*, 29, 135–144, 2002.
- Zubkov, M. V., Tarran, G. A., and Fuchs, B. M.: Depth related amino acid uptake by *Prochlorococcus* cyanobacteria in the Southern Atlantic tropical gyre, *FEMS Microbiol. Ecol.*, 50, 153–161, 2004.
- Zubkov, M. V., Tarran, G. A., and Burkill, P. H.: Bacterioplankton of low and high DNA content in the suboxic waters of the Arabian Sea and the Gulf of Oman: abundance and amino acid uptake, *Aquat. Microbiol. Ecol.*, 43, 23–32, doi:10.3354/ame043023, 2006.